LA-UR-81-1521

TITLE: TRAC-PD2 MODELING OF LOFT AND PWR SMALL COLD-LEG BREAKS

AUTHOR(S): Thad D. Knight
Gordon J. E. Willcutt, Jr.
James F. Lime



SUBMITTED TO: Specialists Meeting on Small-Break
Loss-of-Coolant-Accident Analysis in LWR's
American Nuclear Society
Monterey, California
August 25-27, 1981



University of California
LOS ALAMOS SCIENTIFIC LABORATORY
Post Office Box 1663 Los Alamos, New Mexico 87545
An Affirmative Action/Equal Opportunity Employer

Form No. 836 R3
St. No. 2629
12/78

UNITED STATES
DEPARTMENT OF ENERGY
CONTRACT W-7405-ENG. 36

# TRAC-PD2 MODELING OF LOFT AND PWR SMALL COLD-LEG BREAKS*

by

Thad D. Knight, Gordon J. E. Willcutt, Jr., and James F. Lime

Energy Division
Los Alamos National Laboratory
P.O. Box 1663
Los Alamos, NM 87545

## ABSTRACT

The Transient Reactor Analysis Code (TRAC) is being developed at the Los Alamos National Laboratory to provide advanced best-estimate predictions of postulated accidents in light-water reactors. TRAC-PD2, the latest publicly released version of the code, is currently being tested against small-break and other transients in experimental facilities; it is also being used to analyze postulated accidents in commercial power reactors. Calculated results for LOFT small-break experiments are compared to data, and the results from two small-break calculations for two different reactor systems are presented. We conclude that TRAC-PD2 is useful for the analysis of cold-leg small-break accidents.

* This work was performed under the auspices of the US Nuclear Regulatory Commission.

## I. INTRODUCTION

The Transient Reactor Analysis Code (TRAC) is an advanced best-estimate systems code for analyzing light-water-reactor accidents. It is being developed at the Los Alamos National Laboratory under the sponsorship of the Office of Nuclear Regulatory Research of the US Nuclear Regulatory Commission. TRAC-PD2 (Ref. 1) is the latest in a series of publicly released versions of the code; it features a three-dimensional treatment of the pressure vessel and associated internals, two-phase nonequilibrium hydrodynamics models, flow-regime-dependent constitutive relations, improved reflood tracking capability for both bottom reflood and falling-film quench fronts, improved numerics, and a consistent treatment of the entire accident sequence from the steady-state conditions through reflood. The code is intended primarily for analyzing large-break loss-of-coolant accidents in pressurized water reactors (PWRs); however, the generality incorporated into the thermal-hydraulic modeling permits the code to be applied to a variety of accident scenarios and facilities. In fact, we use the code to study current licensing and safety issues related to potential accidents in PWRs. The initial assessment (Ref. 2) of the code against experiments proceeded concurrently with the development of the code. After release of the code, independent assessment began to test the code's predictive capability.

Below we first discuss a portion of the independent assessment of TRAC-PD2 against Loss-of-Fluid-Test (LOFT) small-break data and then the application of the code to postulated small cold-leg breaks in two PWRs. This process of related assessment and application adds confidence to the application results.

## II. LOFT DATA COMPARISONS

That portion of the independent assessment conducted at Los Alamos includes comparison of the code to experimental data from the LOFT facility. During the past year we have analyzed four of the LOFT small-break tests: L3-1 (Ref. 3), L3-7 (Ref. 4), L3-5 (Ref. 5), and L3-6 (Ref. 6). These four small-break tests provide large-scale integral-system data pertinent to the behavior of PWR systems. The analyses discussed are posttest calculations.

### A. LOFT Facility and Test Descriptions

The LOFT facility is a 50-MW(t) PWR system with a single intact loop containing two active pumps in parallel and an active steam generator. The pressurizer is connected to the hot leg of the intact loop. A single, noncommunicating broken loop contains passive simulators for the pump and the steam generator. This noncommunicating loop does not provide a principal flow path from the hot leg to the cold leg. However, a piping and valve connection (the reflood-assist bypass) between the broken-loop cold and hot legs does exist, but the valves normally are closed. The passive simulators for the pump and steam generator represent the hydraulic resistances with three series of orifice plates and maintain the elevation changes in the intact-loop components. The vessel contains the reactor core, the lower and upper plenums, and the downcomer annulus. The core consists of 1300 fuel rods with

an active length of 1.676 m. The top of the core is below the minimum elevation in the piping loops (the pump suction leg). The facility is instrumented to provide data on the system's thermal-hydraulic behavior during transients.

The break size, its location, and the pump operation were varied from test to test; Table I summarizes the test conditions and the break configuration. In the table, the terminology "noncommunicating, single-ended break" means that there is no principal flow path past the break from the hot leg to the cold leg and that the break is simulated in only one piping leg. Correspondingly, the communicating break does have a principal flow path upstream of the break from the hot leg to the cold leg. The break sizes for tests L3-1, L3-5, and L3-6 represented an equivalent 2.5% break in a commercial PWR, or the rupture of a 4-inch pipe. The break size for test L3-7 represented an equivalent 0.16% break, or the rupture of a 1-inch pipe. All four tests were conducted from steady states with full power and typical primary system fluid conditions.

Test L3-1 simulated the break in the broken-loop cold leg. The reactor was scrammed before initiating the break (at 0.0 s). The pumps were tripped at 0.0 s and coasted down. Normal emergency core coolant (ECC), consisting of the high-pressure injection system (HPIS), the low-pressure injection system (LPIS), and the accumulator, was injected into the intact-loop cold leg based on trip set points typical of a commercial PWR. At 3622 s the operators took control of the facility to return the plant to a stable, safe condition.

Test L3-7 also simulated the break in the broken-loop cold leg. The break was initiated at 0.0 s, and the reactor was scrammed at 36.0 s based on a low-pressure trip signal. The pumps were tripped 3 s later and began to coast down. ECC was limited to HPIS only during the first hour of the transient. The HPIS was initiated based on a normal low-pressure trip and was directed into the intact-loop cold leg. At 1805 s the high-pressure injection was terminated. At 3603 s the plant operators took control to begin plant recovery.

Tests L3-5 and L3-6 are pumps-off and pumps-on tests with the break located in the intact-loop cold leg. The initial phase of each test was conducted in a similar manner with the exception that in test L3-5 the pump trip occurred 0.8 s after the break was initiated and in test L3-6 the pump trip occurred at 2371 s after the break and was based on low system pressure. In both tests the ECC injection was limited initially to HPIS and was directed into the downcomer; late in each test the HPIS was terminated based on a low system-pressure trip, at which time a valve also was closed to isolate the break (terminate break flow). Test L3-5 continued until 5011 s, when the plant operators began plant recovery. In test L3-6 the cladding temperature began increasing rapidly following the pump trip and isolation of the break; the temperature excursion was terminated by initiating both accumulator and high-pressure injection into the downcomer. The plant operators then continued control to recover the plant to a stable, safe condition.

TABLE I

TEST CONDITIONS AND BREAK CONFIGURATIONS
FOR LOFT SMALL-BREAK TESTS

| | LOFT Test | | | |
|---|---|---|---|---|
| | L3-1 | L3-7 | L3-5 | L3-6 |
| Power [MW(t)] | 48.9 | 49.0 | 49.0 | 50.0 |
| Primary-coolant-system flow (kg/s) | 484.0 | 481.3 | 476.4 | 483.3 |
| Hot-leg pressure (MPa) | 14.85 | 14.90 | 14.86 | 14.87 |
| Hot-leg temperature (K) | 574.0 | 576.1 | 576.0 | 577.1 |
| Scram time (s) | -2.15 | 36.0 | -4.8 | -5.8 |
| Pump trip (s) | 0.0 | 39.3 | 0.8 | Delayed |
| Emergency-core-coolant systems | ACC[a] HPIS[b] LPIS[c] | HPIS | HPIS | HPIS |
| Break configuration | | | | |
| Type | NC[d] | NC | C[f] | C |
| Diameter (mm) | 16.18 | 4.04 | 16.19 | 16.19 |
| Length/diameter | 3.34 | 3.51 | 3.33 | 3.34 |
| Location | BLCL[e] | BLCL | ILCL[g] | ILCL |

[a] Accumulator

[b] High-pressure injection system

[c] Low-pressure injection system

[d] Noncommunicating, single-ended break

[e] Broken-loop cold leg

[f] Communicating break

[g] Intact-loop cold leg

## B. TRAC-PD2 Input Model Description

The input model for tests L3-1 and L3-7 consists of 25 components (Fig. 1) with a total of 120 hydraulic cells. For the small-break tests small leakage paths between the hot legs and the cold legs must be modeled; for LOFT the leakages were accounted for by connecting the reflood-assist-bypass lines at junction 43. The break orifice is located in valve component 44. The fully implicit numerics, in combination with a coarse-noding scheme, were used in component 44 to represent the break flow. The break orifice was represented as a flow-area restriction at one interface. The break flow was modeled as friction limited, and the friction at the break orifice was adjusted, once for subcooled fluid conditions and once for saturated fluid conditions, to agree with the Henry-Fauske subcooled-critical-flow model (Ref. 7) and the homogeneous-equilibrium critical-flow model (Ref. 7), respectively.

The vessel was modeled with the three-dimensional vessel component in TRAC; nine axial levels, two radial rings, and two azimuthal segments were used. The core was located in the inner ring, levels 3 through 6. The downcomer was located in the outer ring. The piping connections were made in level 8.

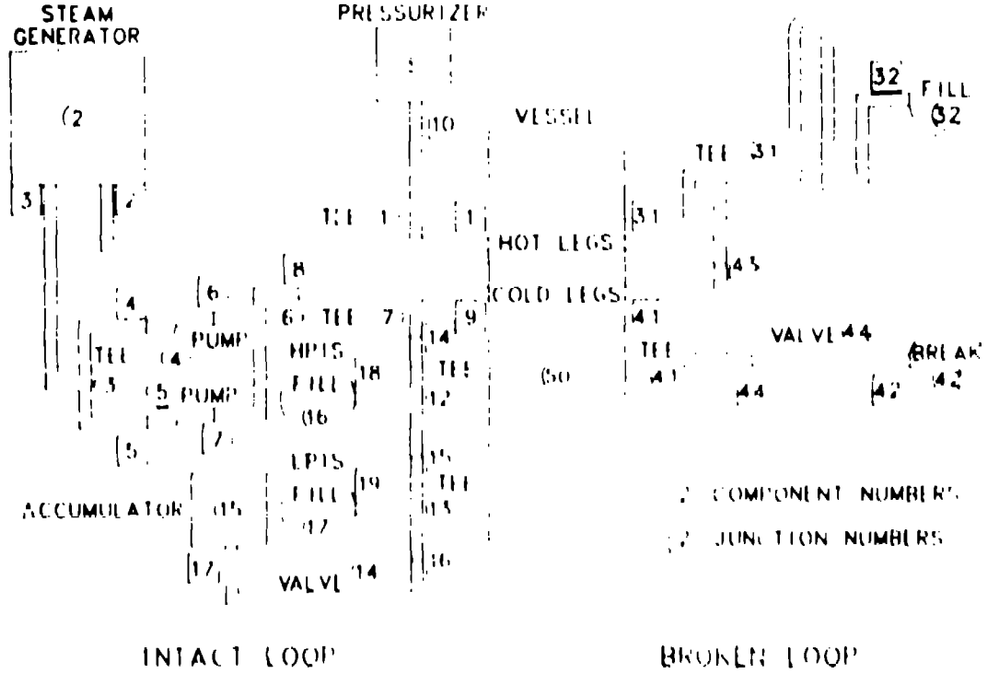


Fig. 1. LOFT system component schematic.

The steam-generator-secondary noding (Fig. 2) has added detail to represent the secondary downcomer. This new noding scheme resulted in the correct secondary liquid inventory and allowed feedwater injection at the correct elevation. Also, the recirculation of fluid up through the tube region of the secondary and down through the downcomer was represented. A new valve type was added to the code to represent correctly the opening and closing of the LOFT steam-flow-control valve. The new valve type also permits the modeling of valve leakage. For tests L3-1 and L3-7, nominal leakage rates were permitted through the steam-flow-control valve.

The total primary-system heat losses were modeled. The heat losses were distributed throughout the one-dimensional components in the primary piping, with the exception of the steam-generator component 2 and the valve component 44. Heat losses were not modeled on the pressurizer component 8 and the components associated with the ECC system.

The semi-implicit numerics were used in all components except valve component 44.

For tests L3-5 and L3-6 the intact-loop cold leg, components 6 and 7, was renoded. Two additional tees, one fill, and one break were required. A tee and fill combination was required to model the injection of coolant through the pumps; the injection was made between the two pumps on the downstream side. A tee and break combination was required to model the intact-loop break

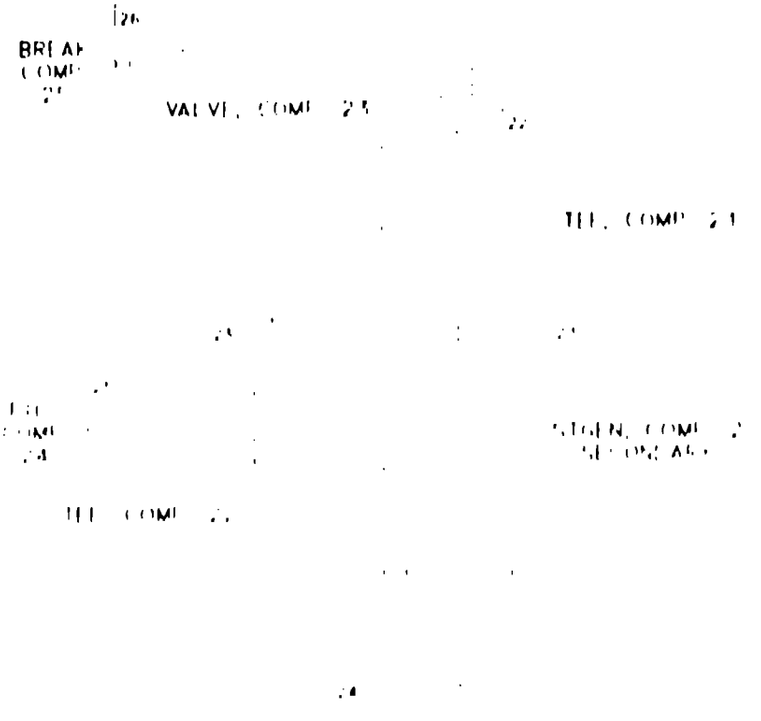


Fig. 2. LOFT steam-generator-secondary noding diagram.

geometry. The first cell in the side leg of the tee leading to the break orifice maintains the correct flow area, but the length of the cell is exaggerated to avoid a Courant time-step limit at the junction with the primary piping leg. The remaining interfaces are treated with fully implicit numerics. The length-to-diameter ratio for the first cell also is correct so that the wall friction is correct. The break orifice is represented as a single cell as opposed to a flow-area restriction at an interface used for tests L3-1 and L3-7. The volume, length, and flow area of the orifice are correct. The wall friction and the additive friction are set to zero, and the hydraulic diameter is set to 1.0 m (this break noding scheme is similar to that used for the application calculations discussed later). Additional cells are used to represent the piping volumes downstream of the orifice. The break was modeled upstream of the intact-loop ECC system. Also, an ECC system, consisting of a pipe component and a fill, was attached to the vessel in level 7, ring 2, azimuthal segment 2. These noding changes increased the number of hydraulic cells to 135.

The analysis for each test consisted of a steady-state calculation and a transient calculation. The steady-state calculations were started from a stagnant, isothermal initial condition and resulted in the desired steady-state conditions for beginning the transients. The calculated conditions are within the data uncertainty of the values given in Table 1. For tests L3-1, L3-5, and L3-6, the scram was assumed to occur at 0.0 s for convenience. For the analysis of test L3-7, the scram and pump coastdown were initiated on a low-pressure trip as in the test.

C. Comparisons To Data

The intact-loop hot-leg depressurization and the break flow for test L3-1 are shown in Figs. 3 and 4. The calculated depressurization is good, although the code began to underpredict the pressure late in the transient. The calculated break flow reflects the trend of the data, but differs in the details as a consequence of the friction-limited nature of the modeling. Even though nominal leakage through the steam-flow-control valve was modeled, TRAC overpredicted the secondary pressure after 100 s. In the calculation the primary-system pressure crosses below the secondary pressure ~100 s before the data indicated the transition; the code then predicted a larger secondary-to-primary pressure differential than the data. TRAC calculated accurately the timing of ECC injection, including the initiation and subsequent emptying of the accumulator (Fig. 5--the discrepancy in initial values represents only differences in the vertical distribution of the same amount of liquid). No dryout of the core was calculated, and none was observed in the data.

Figures 6 and 7 show the intact-loop hot-leg pressure and the break mass flow for test L3-7. The calculated system depressurization is good and shows all of the trends in the data. The underprediction of system pressure at the time the system saturates (~400 s) reflects an inconsistency in the initial hot-leg fluid-temperature data. The calculated break flow also is good but tends to overpredict slightly the data. Figure 8 shows the calculated pressurizer liquid level compared to data. TRAC calculated very well the general trend of the liquid level and the time of emptying. Again, nominal leakage through the steam-flow control valve was modeled. TRAC predicted accurately the secondary pressure; however, between 1000 and 3000 s, the

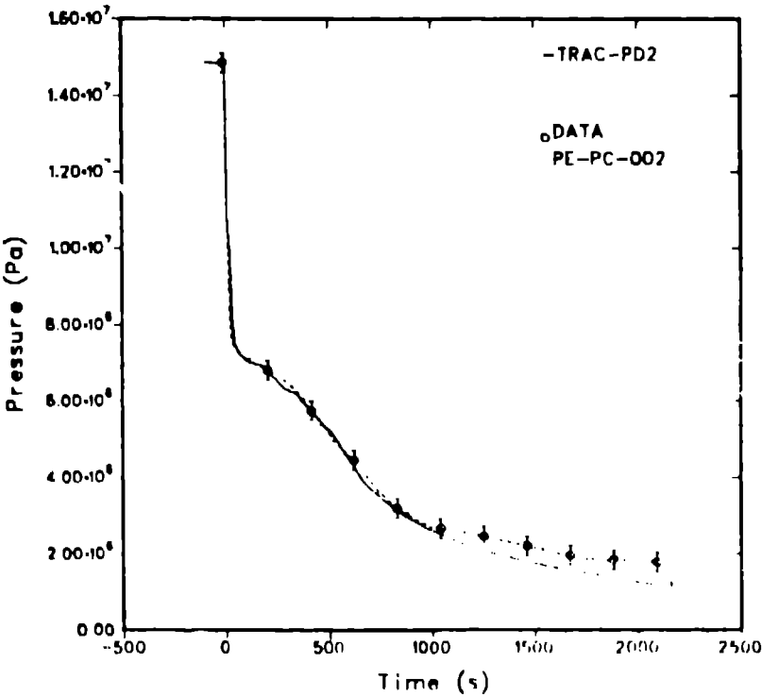


Fig. 3. L3-1 intact-loop hot-leg pressure.

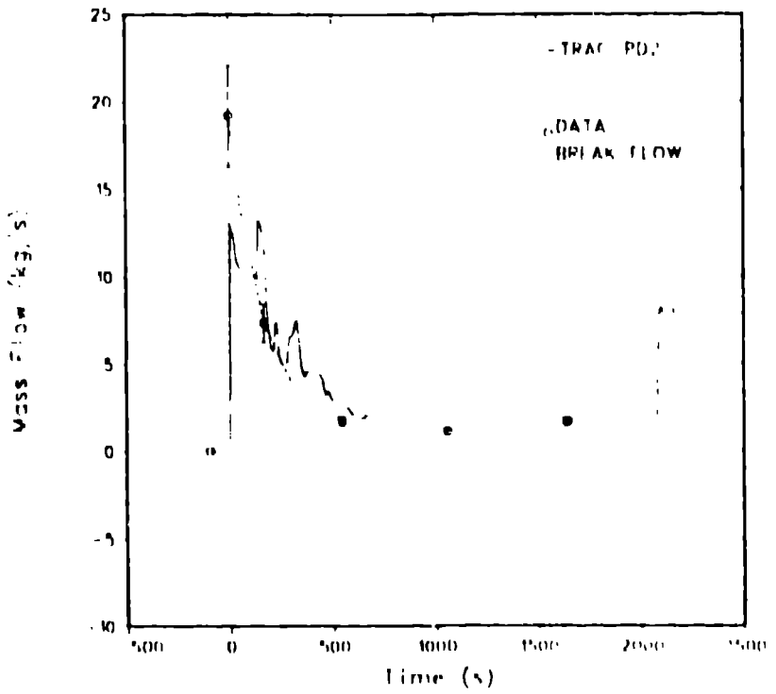


Fig. 4. L3-1 break mass flow.

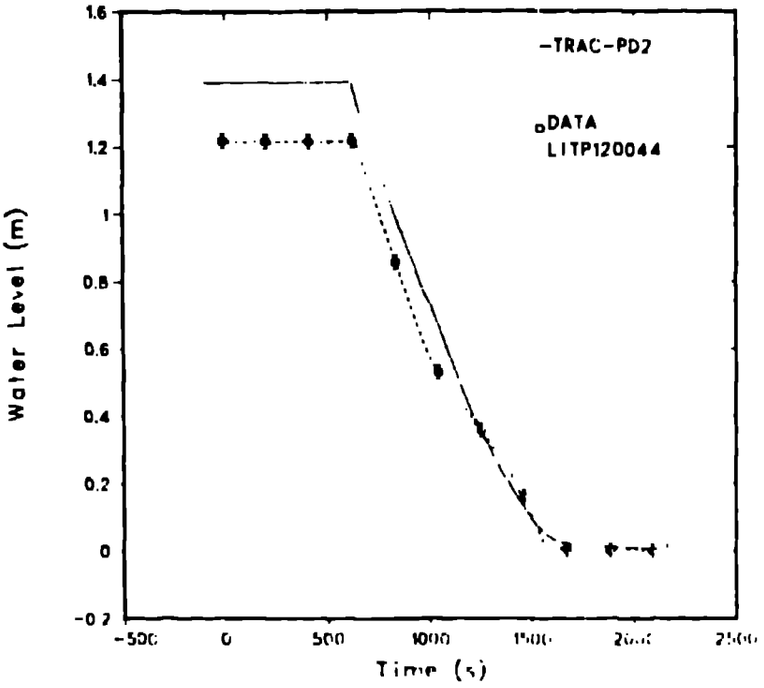


Fig. 5. L3-1 accumulator liquid level.

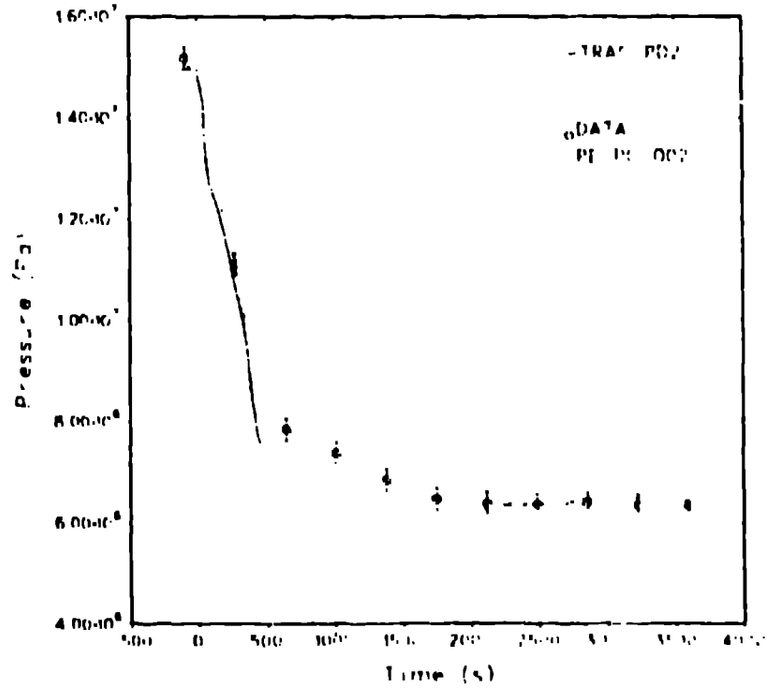


Fig. 6. L3-7 intact-loop hot-leg pressure.

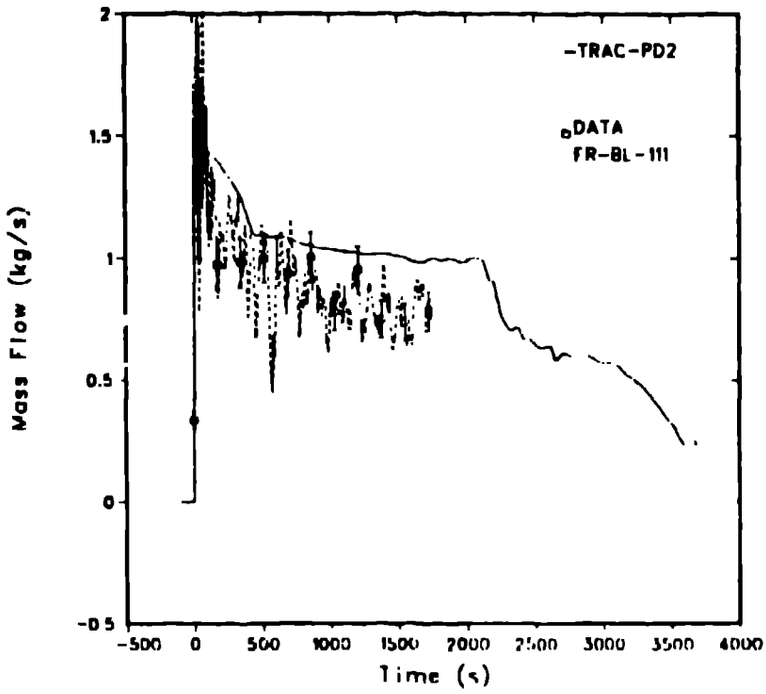


Fig. 7. L3-7 break mass flow.

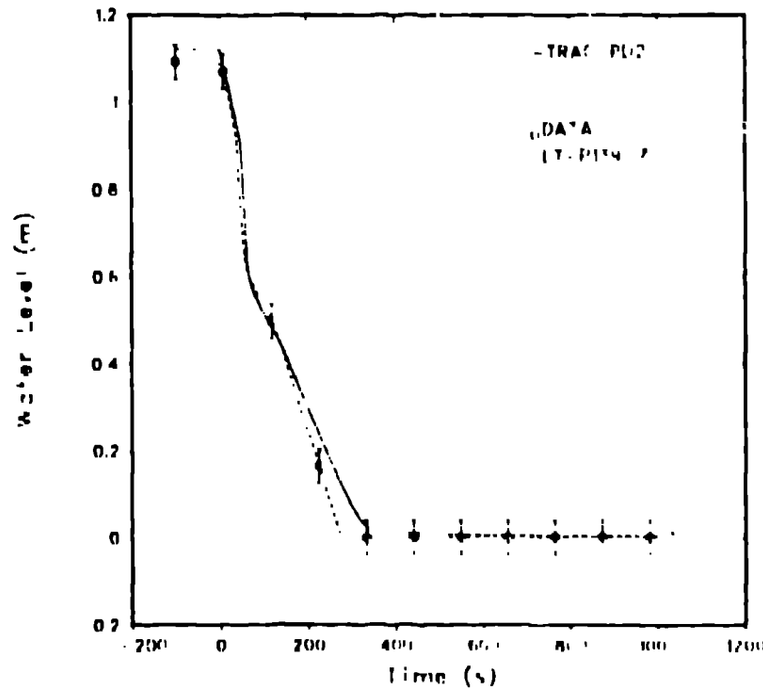


Fig. 8. L3-7 pressurizer liquid level.

secondary pressure was underpredicted slightly. Throughout the 3600 s calculated, the primary-system pressure, both calculated and measured, remained above the secondary pressure. As with test L3-1, test L3-7 demonstrated no core dryout, nor did the code calculate a dryout.

Figures 9 and 10 show the intact-loop hot-leg pressure and the break mass flow for test L3-5, the pumps-off test. TRAC predicted the system pressure very well, although slightly low. Because of this slight underprediction, the break isolation and termination of high-pressure injection occurred ~125 s early at 2185 s. Following isolation of the break, natural circulation was re-established and the system repressurized to above the steam-generator-secondary pressure. The comparison of calculated and measured break flow shows that TRAC predicted the correct trends but may have overpredicted the flow initially. However, during the time that the flow may have been overpredicted, the pressure was also overpredicted, an apparent anomaly. The steam-flow-control-valve leakage was set to zero, but the code underpredicted the secondary pressure between 1000 and 2700 s. The primary system pressure, both calculated and measured, fell below the secondary pressure at ~900 s; but after the break was isolated, the calculated system pressure attained the secondary pressure ~860 s later than occurred in the data. Figure 11 shows the comparison of the calculated and measured cladding temperatures in the central fuel bundle at the high-powered zone. Both temperatures track within a few Kelvin of saturation. Core dryout was neither calculated nor observed.

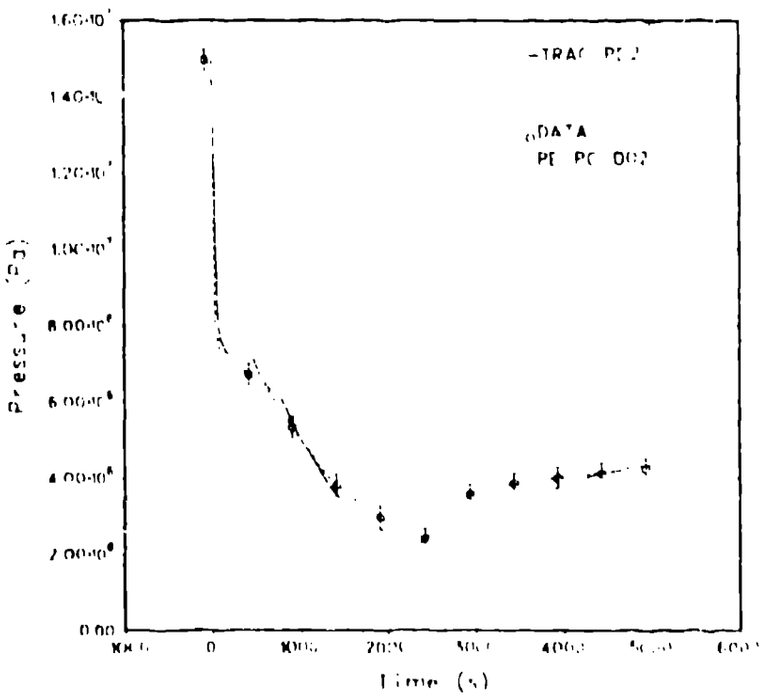


Fig. 9. L3-5 intact-loop hot-leg pressure.

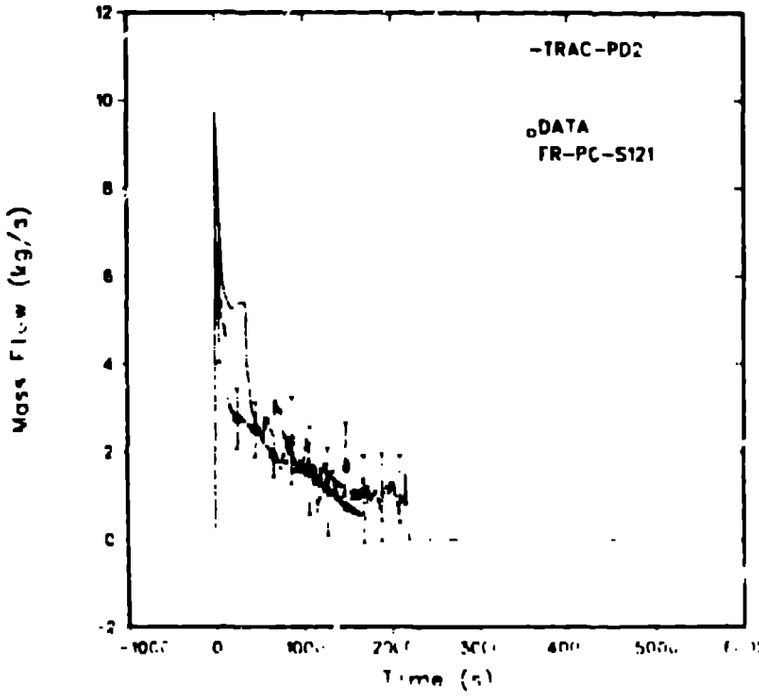


Fig. 10. L3-5 break mass flow.

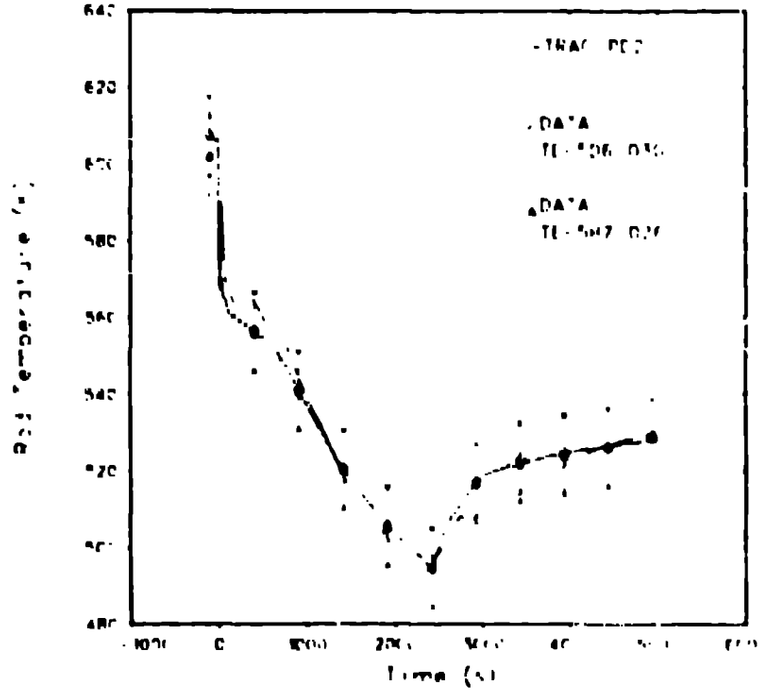


Fig. 11. L3-5 cladding temperature in the central fuel bundle at the elevation of maximum power.

Test L3-6 intact-loop pump-suction-leg pressure and break flow are shown in Figs. 12 and 13. The primary-system pressure was calculated accurately. Because of uncertainty in the low-system-pressure set point and of a very small overprediction of the pressure, the timing of the pump trip was predicted to occur at 2691 s, 320 s later than the data. The timing of the isolation of the break and the re-establishment of ECC were based on elapsed time after the low-system-pressure trip. TRAC predicted very well the break flow; while this calculation did not show the flow spike just before isolating the break, a similar spike was calculated for test L3-5 (Fig. 10). The steam-generator-secondary pressure comparison was good for the first 1000 s, at which time the measured secondary and primary pressures began to diverge; this divergence occurred at ~1800 s in the calculation. This timing discrepancy indicated that the code maintained close thermal coupling between the primary and secondary much longer than the test. Figure 14 shows the cladding temperature comparisons in the central fuel bundle at the elevation of maximum power. Following the pump trip and during the coastdown, both a calculated and a measured temperature excursion occurred throughout the core. The temperature excursion was terminated by the initiation of full ECC injection into the downcomer. TRAC predicted this excursion extremely well, including the magnitude of the excursion. The difference in the timing of the excursion between the data and the calculation reflects only the difference in timing of the pump trip.

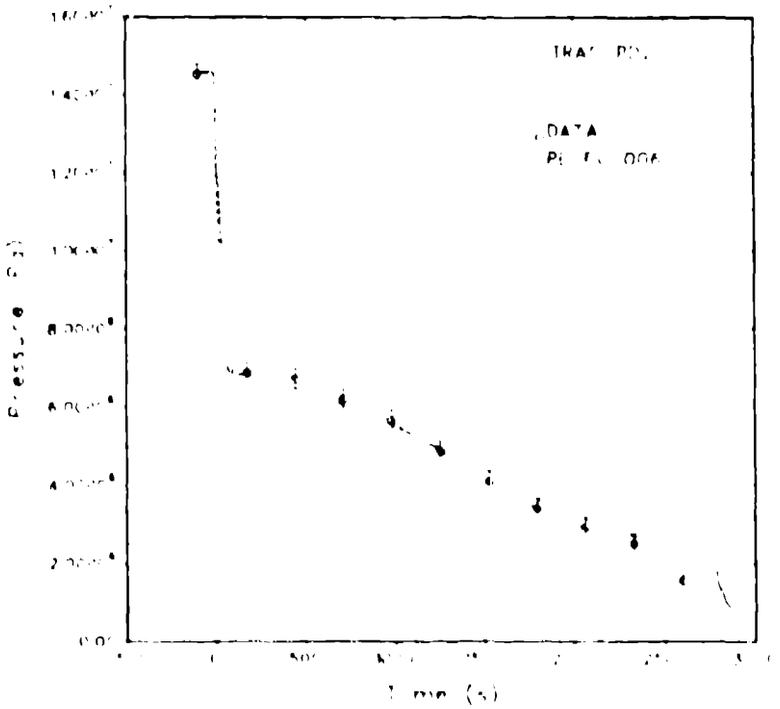


Fig. 12. L3-6 intact-loop pump-suction-leg pressure.

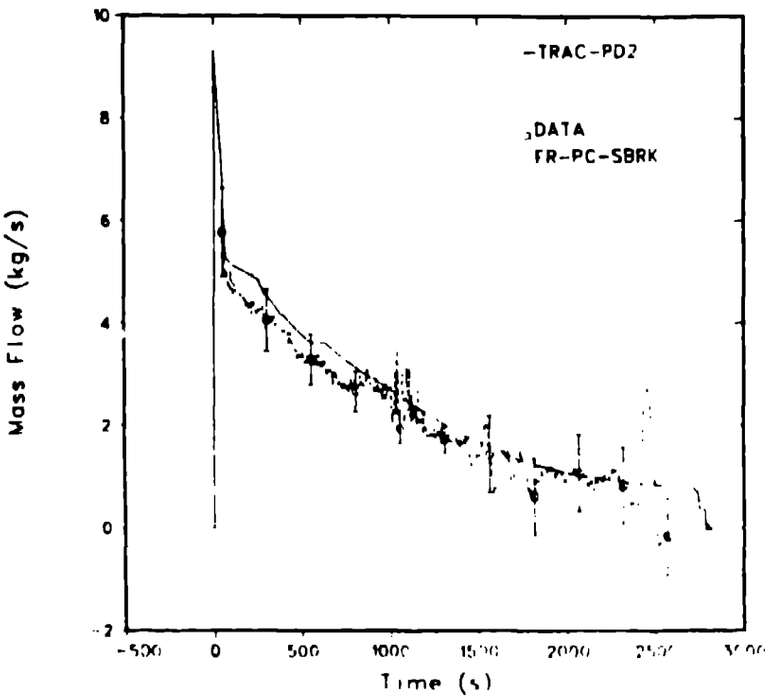


Fig. 13. L3-6 break mass flow.

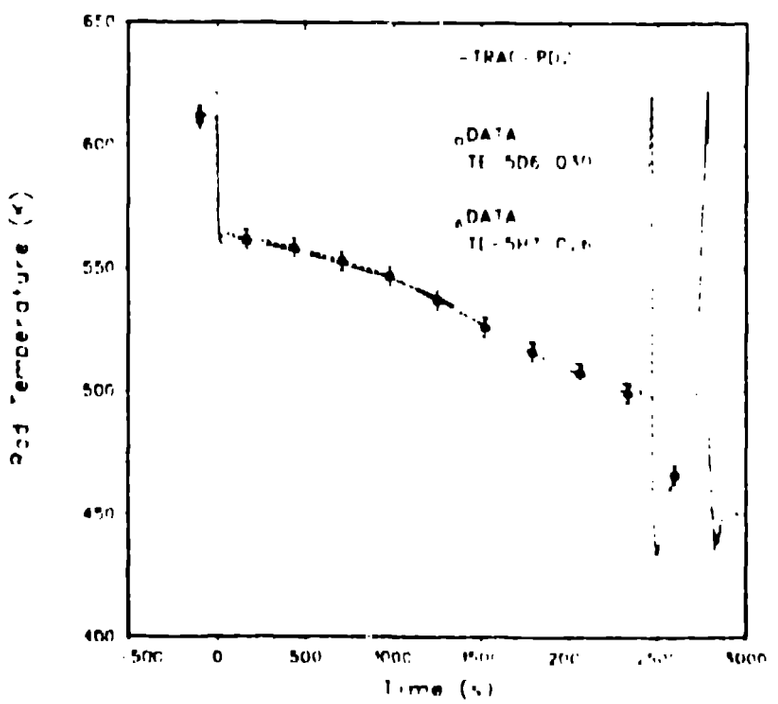


Fig. 14. L3-6 cladding temperature in the central fuel bundle at the elevation of maximum power.

TRAC-PD2 provides a useful small-break modeling capability for predicting most thermal-hydraulic phenomena during slow transients. In particular, the code correctly predicted, in posttest analyses, the behavior of four different LOFT small-break tests in which break size and location and pump operation were varied. The calculated liquid-mass distributions generally were consistent with the data. There were no significant mass-conservation errors. Improved critical-flow modeling is needed, either in improved constitutive relations or in a critical-flow model. Both of these paths are being explored as a part of the current TRAC development effort (TRAC-PF1). Finally, small-break analysis requires detailed definitions of the flow paths, including the leakage paths, and measurements for all important flows are desirable when assessing the code's predictive capability.

## III. PWR SMALL COLD-LEG BREAKS

The remainder of this paper describes results from the first extensive application of TRAC-PD2 to predict system behavior for postulated small cold-leg breaks in US PWRs. Los Alamos has run several small cold-leg break transients for a Babcock and Wilcox (B&W) lowered-loop plant (TMI-2), a 5% raised-loop plant (Davis-Besse), and a Westinghouse four-loop plant (Zion-1). Examples are presented here for a 0.00093-$m^2$ (0.01-$ft^2$) break in the TMI-2 model that does not produce loss of natural convection and a 0.0 1[illegible]-$m^2$ (0.02-$ft^2$) break in the Zion-1 model that does produce complete loss of natural convection. This work is being performed for the Nuclear Regulatory Commission's Office of Nuclear Reactor Regulation to aid them in assessing vendor calculations of small cold-leg breaks.

In addition, we are calculating other transients with TRAC including overcooling, undercooling, steam generator tube ruptures, and the effects of delayed pump trips for small cold-leg breaks. We also are performing TRAC benchmark calculations by comparing calculated results with actual plant transients.

These PWR applications used the TRAC-PD2 code with the following additional features. For our B&W applications, we added a vent valve model to the vessel and an auxiliary feedwater system to the steam generator with control based on a steam generator level calculation and/or operator actions. The auxiliary feedwater system model permits the flow to enter near the top of the steam generator. We also improved the modeling of the mixing of liquid and vapor between one-dimensional cells in horizontal and vertical flow regimes for the very low flow rates encountered with small-break transients. The TRAC version used also included several other improvements and corrections to the TRAC-PD2 code.

We modeled the small break using a tee component with a large-area junction between the side tube and the cold leg to avoid Courant time step limitations at the junction. The flow area in the fully implicit side tube was reduced in the first cell from the large junction area to the actual break area. The second cell in the side tube had an area equal to the break area and a length equal to the wall thickness. A break component at atmospheric pressure was attached to the end of the side tube. The results of this small-break model reproduce the results from critical-flow models for both the subcooled and saturated regions.

## A. TMI-2 Model Description

Figure 15 is a sketch of the TRAC model for the TMI-2 reactor system. Loop A represents the loop with the cold-leg break. It includes the hot leg with the pressurizer connection, the steam generator, and two cold legs--one intact and one with the 0.00093-$m^2$ (0.01-$ft^2$) break. Each loop-A cold leg includes a loop seal, a pump, and a high-pressure injection (HPI) location. The secondary side of the steam generator is attached to the main feedwater inlet, the auxiliary feedwater inlet, and a long pipe to the steam outlet with a side connection to a safety valve that vents to the atmosphere.

Loop B represents the unbroken loop. It is similar to loop A except there is no break or pressurizer and the two cold legs are combined to increase calculational efficiency.

We noded the vessel with four azimuthal segments, two radial segments, and seven levels. The seven levels included a lower plenum, three active core levels, two levels in the upper plenum (to permit the vent valves to be above the hot and cold leg connections), and an upper head. In addition to the 56 three-dimensional vessel cells, there are 113 one-dimensional cells, 89 in the primary and 24 in the secondary side. Geometry and other plant data were obtained from the TMI-2 Final Safety Analysis Report (FSAR) and other TMI-2 data sources.

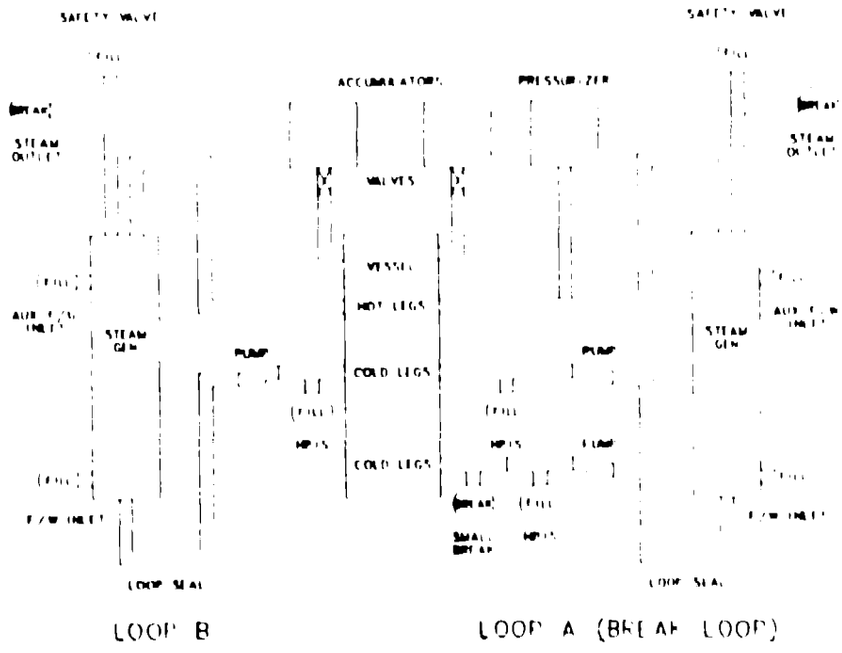


Fig. 15. TRAC model of TMI-2 PWR.

## B. TMI-2 Calculation Results

We have modeled 3600 s of this transient starting from 102% of steady-state power with the break assumed to occur at the initial time in the transient. At 72 s, the reactor tripped when the pressure decreased to 13.1 MPa (1900 psia), and the reactor coolant pumps and main feedwater pumps also were tripped at this time. After a delay of 40 s from the reactor trip time, the auxiliary feedwater was initiated to both steam generators. At 184 s, the primary pressure decreased to the HPI set point of 9.41 MPa (1365 psia), and the HPI was turned on. This HPI set point is based on the design value minus tolerances.

As shown in Fig. 16, the primary pressure decreased rapidly until ~775 s, at which time the steam generator level reached 50% of the operating range, and the auxiliary feedwater then was turned off. Subsequently, almost all the cooling resulted from the HPI system, and the water level never dropped enough in either steam generator to turn on the auxiliary feedwater system again. Both the primary and secondary pressures rose slightly after the auxiliary feedwater was turned off, but they began to decrease again before the end of the 3600 s modeled. After 425 s, the combined HPI flow to all cold legs (Fig. 17) exceeded the break flow for the remainder of the transient.

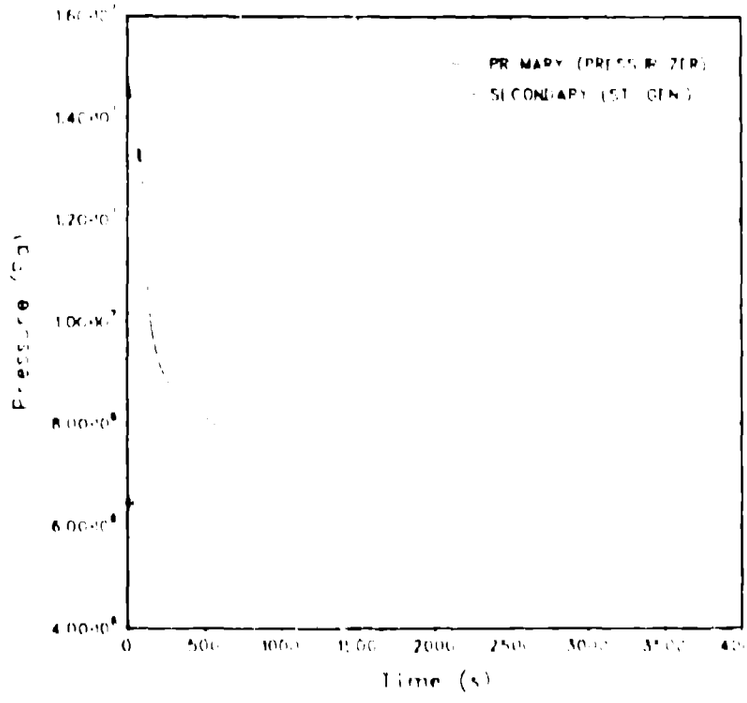


Fig. 16. TMI-2 primary and secondary pressures.

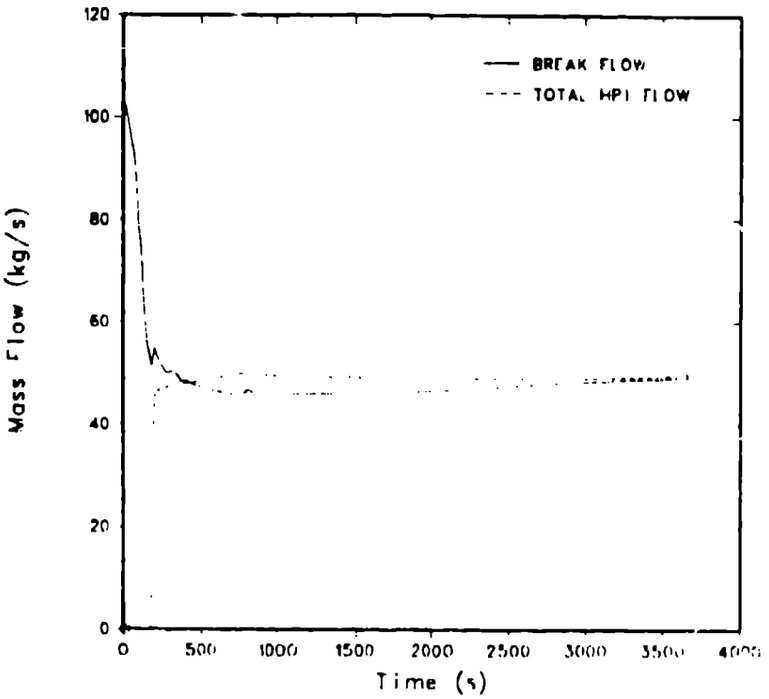


Fig. 17. TMI-2 break flow and total HPI mass flow.

Figure 18 shows the mass flow for the combined cold legs in the unbroken loop; the flow rapidly decreased to ~1000 kg/s by 300 s and remained above 950 kg/s for the remainder of the transient. The flow in the loop-A cold leg was approximately half the amount shown in Fig. 18. The core remained covered with water for this entire transient, and the peak cladding temperature never exceeded the initial value.

## C. Zion-1 Model Description

Figure 19 shows a sketch of the TRAC model for the Zion-1 reactor system. The 0.00186-$m^2$ (0.02-$ft^2$) break is located in the cold leg of loop B, downstream of the pump and safety injection point. The pressurizer also is located in loop B. The three intact loops are modeled as one combined loop, referred to as loop ACD in this analysis. We divided the vessel into eight axial levels, two azimuthal segments, and two radial rings. The core was modeled with four axial levels. On the secondary side of the steam generators, we modeled the steam lines leading outside the containment building and the secondary safety valves; we also modeled the primary loop seals between the steam generator outlets and the primary coolant pumps. There are a total of 32 three-dimensional vessel cells and 132 one-dimensional cells, 80 in the primary and 52 in the secondary side. Geometry and other plant data were obtained from the Zion-1 FSAR and from other Zion-1 data sources.

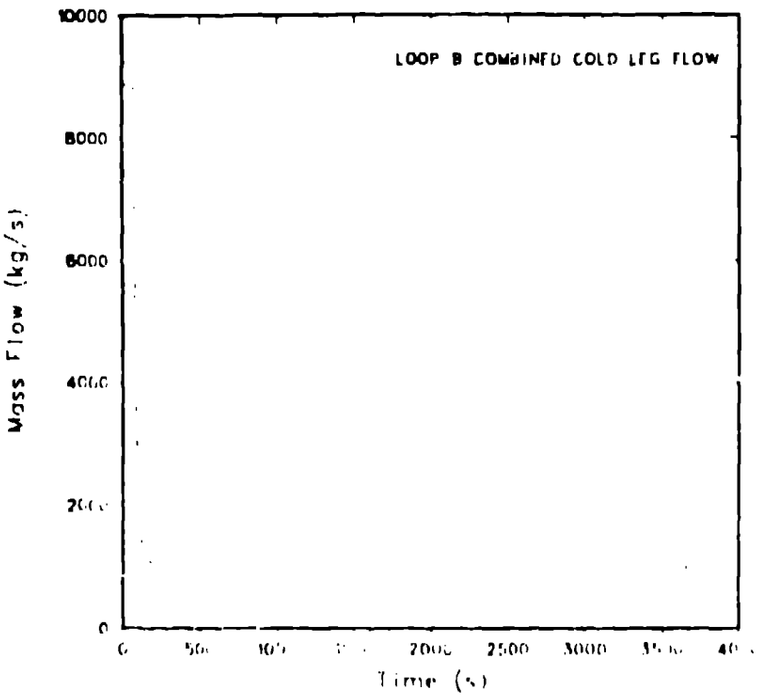


Fig. 18. TMI-2 loop-B cold-leg mass flow.

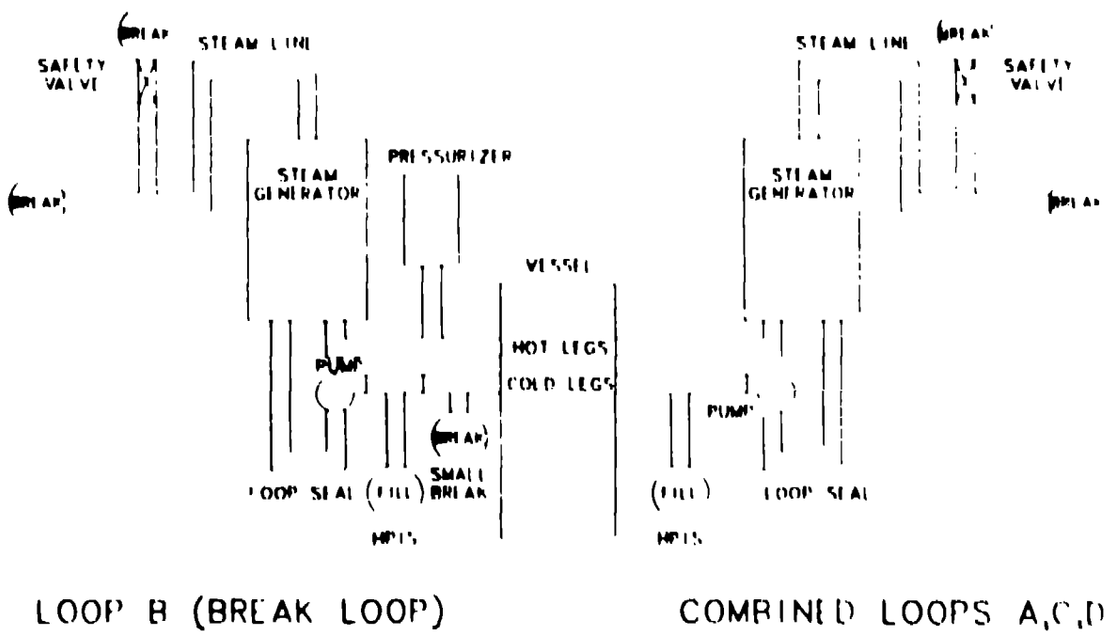


Fig. 19. TRAC model of Zion-1 PWR.

## D. Zion-1 Calculation Results

We assumed a break size of 0.00186 $m^2$ (0.02 $ft^2$) and loss of off-site power at reactor trip time. The loss of offsite power results in an immediate trip of the primary pumps, loss of main feedwater, closing of the turbine stop valves, and availability of only half the safety injection and auxiliary feedwater systems. We calculated the transient out to 5000 s. Table II summarizes the significant events of the transient.

Figure 20 shows the pressurizer and steam generator secondary pressures. The transient was characterized by a rapid depressurization of the primary system in the first 500 s. Between 500 and 1500 s, the pressure temporarily stabilized at slightly above the steam generator secondary pressure. The steam generator secondary pressure rapidly increased to the secondary safety valve set point following loss of main feedwater at the reactor trip time and remained near that level from 150 s until ~1700 s. At 1500 s, the primary pressure began to increase until the primary loop seal in the combined A/C loop cleared of liquid at ~2100 s. After the loop seals cleared, the primary

TABLE II

Zion-1 TRANSIENT EVENTS

| | Event | Time (s) |
|---|---|---|
| 1. | Break occurs. | 0.0 |
| 2. | Reactor trip signal, RCS pumps trip, loss of feedwater, and turbine stop valves close. | 69.1 |
| 3. | Reactor scrammed. | 69.2 |
| 4. | Safety injection flow initiated. | 94.1 |
| 5. | Auxiliary feedwater flow initiated. | 129.1 |
| 6. | Steam-generator safety valves open. | 156.0 |
| 7. | Primary loop seals clear. | 2100.0 |
| 8. | Auxiliary feedwater flow stopped. | 3129.0 |
| 9. | Primary pressure drops below secondary pressure. | 3500.0 |
| 10. | Vessel liquid-mass inventory starts to increase. | 3700.0 |
| 11. | Safety injection flow exceeds break flow. | 4200.0 |

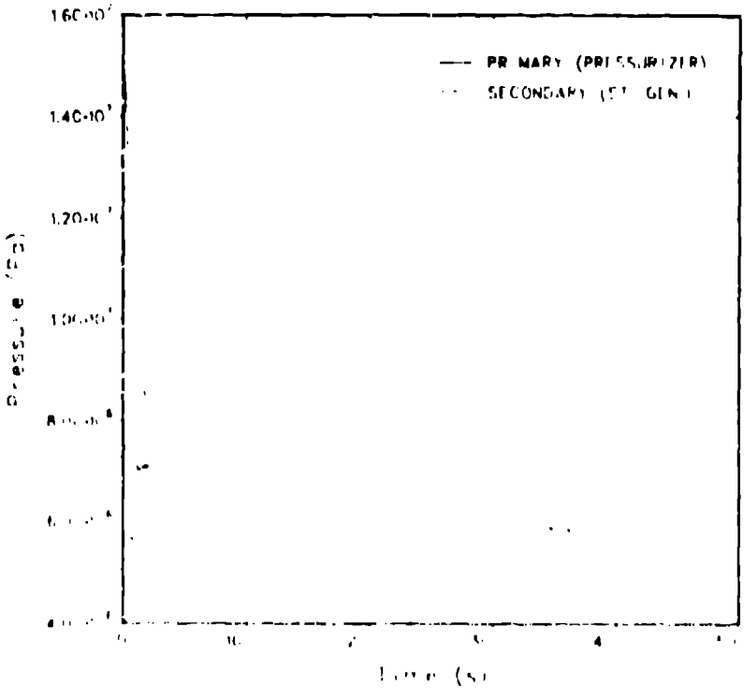


Fig. 2 . Zion-1 primary and secondary pressures.

system gradually depressurized throughout the rest of the transient. The secondary pressure also decreased until the auxiliary feedwater was turned off at 3129 s, after 3000 s of operation. The secondary pressure then remained relatively constant at ~5.9 MPa for the rest of the transient.

Figure 21 shows the void fractions in the upper two levels of the core and in the upper plenum. The void fraction in level 6, the top level of the core, remained well below 0.4 except for a brief period between 2200 s and 2400 s, during which it peaked at 0.68. To determine whether any core uncovery occurred, we renoded the top core level into three smaller levels and recomputed the transient between 2000 s and 2500 s. In the renoded case, the void fraction in the topmost core level never exceeded 0.8. The peak cladding temperature never exceeded the initial value during the transient.

Figure 22 shows the break flow and the total safety injection flow. The safety injection flow began exceeding the break flow at ~4200 s. However, condensing steam actually began increasing the vessel liquid-mass inventory at ~3700 s.

The clearing of liquid in the primary loop seals had an important effect. Before loop-seal clearance, the break flow was essentially all liquid, which resulted in a high mass loss. Once the loop seals cleared, an open path was formed between the core upper plenum and the break, allowing the upper-plenum high-vapor mixture to escape and exit out the break. The path was not a direct one because the loop seal in the broken loop never cleared. Instead,

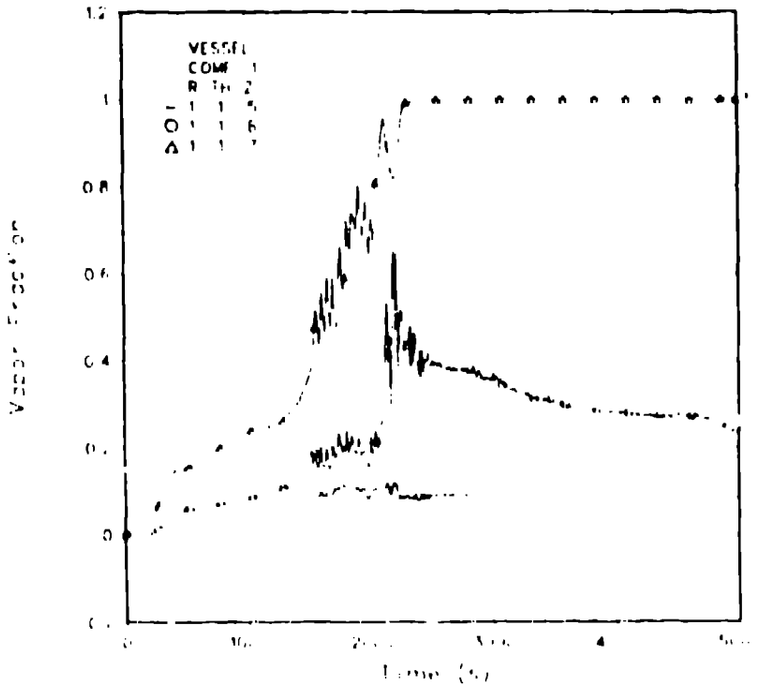

Fig. 21. Zion-1 core and upper-plenum void fractions.

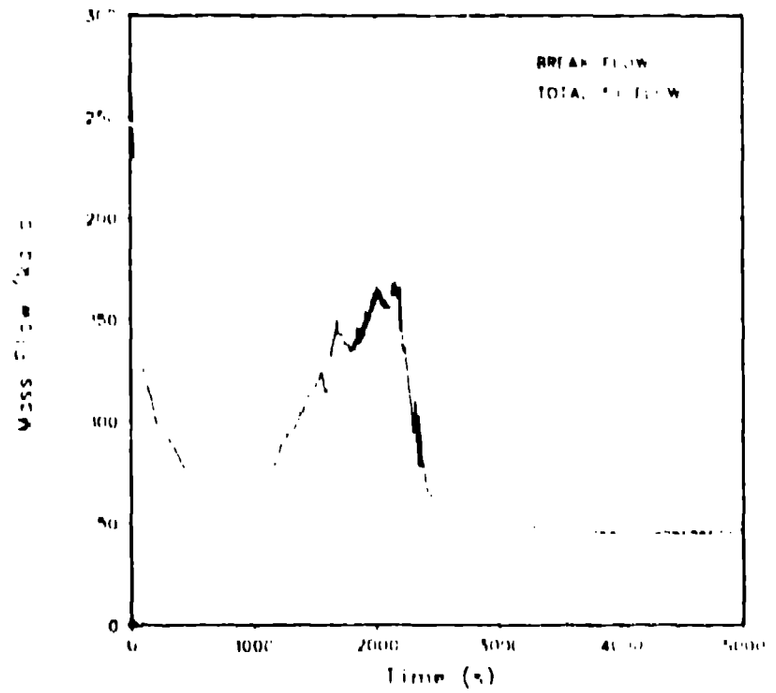


Fig. 22. Zion-1 break flow and total safety injection mass flow.

the flow escaped through the intact loops, through the downcomer annulus, and into the broken cold leg from the vessel side. The highly voided condition near the break resulted in a marked decrease in break mass flow and an increase in the rate of depressurization.

Flow circulation ceased at ~2200 s in loop ACD (Fig. 23) except for the upper-plenum vapor flow escaping out the break. Flow was never re-established in loop B because the loop seal in that loop never cleared. This same phenomenon was observed in Semiscale Test S-SB-P1 (Ref. 8).

## IV. CONCLUSIONS

TRAC-PD2 provides a good, versatile small-break modeling capability. The results above for LOFT show that the code can predict most important phenomena occurring in small cold-leg breaks. In particular, the depressurizations and break flows compared well with data. The good comparisons with the cladding temperatures, both when the core did not uncover and when it did, indicate the vessel liquid-mass inventories were reasonable.

In the applications area, two different accident scenarios were modeled in two different PWRs. In one case natural circulation was maintained, and in the other natural circulation was lost. In both cases the cladding temperatures never rose above the initial values.

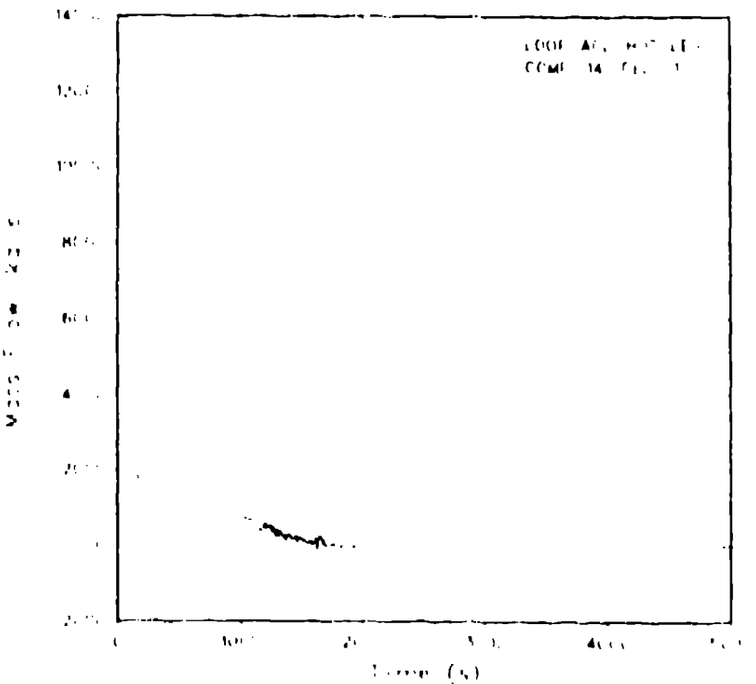

Fig. 23. Zion-1 loop-ACD mass flow.

The addition of a critical-flow model, or improvements to the constitutive relations for the case of large spatial gradients, would simplify the application of the code to small breaks. Also, in certain cases a horizontal-slip model with counter-current flow capability would be beneficial. The TRAC-PF1 development group is addressing these needs. Finally, all small leakage paths should be modeled.

## REFERENCES


1. "TRAC-PD2: An Advanced Best-Estimate Computer Program for Pressurized Water Reactor Loss-of-Coolant Accident Analysis," Los Alamos National Laboratory report LA-8709-MS (to be published).

2. J. C. Vigil and T. D. Knight, "TRAC Development and Assessment Status," Proc. Conf. on Simulation Methods for Nuclear Power Systems, Tucson, Arizona, January 25-28, 1981 (to be published).

3. Paul D. Bayless, J. Bruce Marlow, and Rahland H. Averill, "Experiment Data Report for LOFT Nuclear Small Break Experiment L3-1," EG&G Idaho, Inc. report EGG-2007, NUREG/CR-1145 (January 1980).

4. Dawn L. Gillas and Janice M. Carpenter, "Experiment Data Report for LOFT Nuclear Small Break Experiment L3-7," EG&G Idaho, Inc. report EGG-2060, NUREG/CR-1570 (August 1980).

5. Leanne Thuy Lien Dao and Janice M. Carpenter, "Experiment Data Report for LOFT Nuclear Small Break Experiment L3-5/L3-5A," EG&G Idaho, Inc. report EGG-2060, NUREG/CR-1695 (November 1980).

6. Paul D. Bayless and Janice M. Carpenter, "Experiment Data Report for LOFT Nuclear Small Break Experiment L3-6 and Severe Core Transient Experiment L8-1," EG&G Idaho, Inc. report EGG-2075, NUREG/CR-1868 (January 1981).

7. "RELAP4/MOD5: A Computer Program for Transient Thermal-Hydraulic Analysis of Nuclear Reactors and Related Systems; User's Manual," Vol. 1, Aerojet Nuclear Company report ANCR-NUREG-1335 (September 1976).

8. I. L. Weidert and L. B. Clegg, "Experiment Data Report for Semiscale Mod-3 Small Break Series (Tests S-SB-P1, S-SB-P2, and S-SB-P7)," EG&G Idaho, Inc. report EGG-2053, NUREG/CR-1640 (September 1980).